Check for updates

A novel approach to achieve Os isotope equilibration under ambient conditions for negative thermal ionization mass spectrometry (N-TIMS) analysis

Jin-Hua Liu, [iD] [a] Xiao-Dong Deng,*[a] Jian-Wei Li,[ab] Lan-Ping Feng [iD] [a] and Thomas J. Algeo [iD] [acde]

The rhenium–osmium (Re–Os) isotopic system has emerged as a widely utilized tool in cosmochemistry and high-temperature geochemical studies. A critical prerequisite for high-precision Os isotope analysis *via* Negative Thermal Ionization Mass Spectrometry (N-TIMS) involves achieving complete isotopic equilibrium between the sample and spike through the isotope dilution technique. In this study, we present an innovative technique to address valence state disparities in Os species within mixed solutions, thereby enabling effective isotopic equilibration through a chemical reducing reaction with a strong reductant under ambient conditions. Experimental results demonstrate that a solution containing 0.05 mol L^{-1} hydroxylamine hydrochloride ($NH_2OH \cdot HCl$) coupled with 0.01 mol L^{-1} HBr effectively stabilizes a nanogram-level Os mass. Systematic optimization of reductant concentration and sample-to-reductant ratio yielded a mean $^{190}Os/^{188}Os$ value of 1.2280 ± 0.0006 (2s, $n = 18$) for a mixed Os spike solution, closely aligned with the recommended value of 1.2278 ± 0.0003 (2s, $n = 12$) obtained through the conventional Carius tube method. Controlled comparative experiments revealed critical considerations for method implementation: (1) a freshly prepared reductant must be employed immediately to ensure reagent efficacy, and (2) precise absolute volume control of the reductant solution is essential to mitigate potential losses of volatile OsO_4 linked to extended decomposition times. This novel approach successfully achieves isotopic equilibration between sample–spike and inter-spike components under ambient conditions, offering significant analytical advantages over traditional methods. The validity of the proposed approach was demonstrated by analyzing reference material WMS-1a yielding a $^{187}Os/^{188}Os$ value of 0.1665 ± 0.0006 (2s, $n = 5$), which agrees within uncertainty with the established value of 0.1664 ± 0.0003 (2s, $n = 5$) obtained *via* the Carius tube method. The protocol enhances operational efficiency by reducing equilibration time and explosive risk, and decreases procedural Os blanks *via* reducing material and reagent consumption. The combined improvements in precision, cost-effectiveness, and methodological flexibility position this technique as a valuable advancement in Os isotope geochemistry.

1 Introduction

Both osmium (Os) and rhenium (Re) are highly siderophilic (iron-loving) and chalcophilic (sulfur-loving) elements, exhibiting a strong affinity to partition into sulfide phases.[1,2]

[a]State Key Laboratory of Geological Processes and Mineral Resources, China University of Geosciences, Wuhan 430074, China. E-mail: dengxiaodong@cug.edu.cn

[b]School of Earth Resources, China University of Geosciences, Wuhan 430074, China

[c]State Key Laboratory of Geomicrobiology and Environmental Changes, School of Earth Science, China University of Geosciences, Wuhan 430074, China

[d]Department of Geosciences, University of Cincinnati, Cincinnati, Ohio 45221-0013, USA

[e]State Key Laboratory of Oil and Gas Reservoir Geology and Exploitation, Chengdu University of Technology, Chengdu 610059, China

Consequently, sulfide minerals have emerged as an ideal target for Re–Os isotopic dating and geochemical investigations.[3–5] The $^{187}Re–^{187}Os$ decay systems therefore have gained significant importance as chronometers and tracers in studies related to planetary differentiation,[6,7] mantle heterogeneity,[8–11] crust–mantle interactions,[12–14] and the formation of economically significant ore deposits.[15–21] A critical preparatory step for high-precision Os isotope analysis *via* Negative Thermal Ionization Mass Spectrometry (N-TIMS) is the isotope dilution technique, involving spike addition followed by complete spike–sample equilibration.[22–24] However, the equilibration between the sample and spike is a widespread and persistent issue that has long posed a significant challenge for Os isotope analysis.[18,25–29] Established digestion protocols include the Carius tube and

high-pressure asher (HPA) methods, which commonly facilitate simultaneous sample digestion and spike equilibration in oxidizing media (*e.g.*, inverse *aqua regia*) at elevated temperatures (>230 °C).[30,31] Alternative approaches such as the nickel sulfide (NiS) fire assay and alkali fusion have been employed for bulk sample processing in Re–Os studies.[32–34] However, complete spike–sample equilibration is not stable due to relatively complex operations and required attention.[27] For example, a limited volume of the Os spike can avoid the solution contacting the crucible wall, which may absorb the spike solution.[27] Therefore, improved and modified alkaline fusion methods were developed.[27,35–37] However, the drawback for the NiS fire assay is the elevated procedural blanks.[23] Additionally, the operational envelope of Carius tube digestion is methodologically constrained to <0.5 g aliquots, as larger sample masses induce progressive pressure buildup from accelerated sulfide-acid reactions, increasing rupture probability beyond acceptable safety thresholds.[30] To reduce that risk, large masses of samples should be first dissolved in HNO_3 to release OsO_4 to be trapped by 10 mol L^{-1} HCl in an ice-water bath and subsequently transferred into a Carius tube at 200 °C for the necessary equilibration of trapped Os with a spike under high-temperature and high-pressure conditions.[38]

The incomplete equilibration of Os isotopes between the sample and spike (or inter-spike analyte, as in the present study) is likely related to their variable oxidation states,[39] which introduces significant challenges for N-TIMS analysis (as observed in the present study) generally offering superior analytical performance owing to its high ionization efficiency (3–20%) and negligible memory effects.[40] To mitigate the effects of valence discrepancies between the sample and spike, addition of a strong reducing reagent ($NH_2OH \cdot HCl$) was proposed to achieve the effective equilibration of Os isotopes. Systematic optimization of reagent concentration and sample loading protocols demonstrates that the use of $NH_2OH \cdot HCl$ effectively achieves spike–sample equilibration through chemical reductive reaction under ambient conditions, eliminating the need for the high-temperature Carius tub method. Comparative analyses against conventional methods confirm equivalent measurement results in Os isotope ratios at intermediate precision. The developed protocol successfully applied to Os isotope analysis for reference material WMS-1a addresses two persistent challenges in Re–Os geochronology: (1) reducing the procedural blanks by minimal use of consumable materials and reagents associated with traditional acid digestion, particularly critical for low-abundance Os samples; and (2) enhancing laboratory safety and throughput by limiting the equilibrating time under ambient conditions, establishing a robust framework for high-precision analysis of Os isotopes measured on N-TIMS.

2 Experimental protocols

2.1 Reagents and materials

Laboratory-grade HNO_3, HCl, and HBr from Sinopharm were purified twice using a DST-1000 acid purification system (Savillex, USA; 4 L capacity) *via* sub-boiling distillation at 80 °C,

and heating automatically ceased when the residual volume reached 0.5 L. Prior to HNO_3 distillation, a mixed solution of 30% H_2O_2 and HNO_3 (1 : 4, v/v) was sub-boiled on a hot plate to minimize the Os blank, following Yang *et al.* (2015).[41] Ultra-pure H_2SO_4 (99.9999%, Macklin) was used directly for Os powder digestion and oxidant preparation with Cr_2O_3 (Macklin). Ammonium osmate chloride (99.99%, Aladdin) was used for standard solution preparation, while $NH_2OH \cdot HCl$ (analytical grade, Aladdin) served as a reductant for Os isotope equilibration.

The ^{190}Os and ^{188}Os spike powders (ISOFLEX, USA) were digested in a H_2SO_4–HNO_3 mixture for double spike preparation. High-purity Pt ribbons (99.995%, 0.04 mm thickness, 0.70 mm width, Thermo Fisher Scientific, USA) were used for sample loading, and ultrapure water (18.2 MΩ cm, Millipore Corp., USA) was used for acid dilutions. A reference material WMS-1a (massive sulfide) from the Canadian Certified Reference Materials Project (CCRMP) was used to validated the efficacy of the proposed approach.

2.2 Sample preparation

The Os content in $(NH_4)_2OsCl_6$ often deviates from its theoretical value, necessitating the preparation of a standard Os solution using the precise gravimetric method described by Markey *et al.* (2007).[42] The enriched powders (^{188}Os and ^{190}Os) were combined with 30 mL of 1 : 1 (v/v) H_2SO_4 and HNO_3 in a 500 mL round-bottom flask secured in a 100 °C heating mantle. Evolving OsO_4 vapor was directed through PFA tubing to ice-bath concentrated HBr (8.8 mol L^{-1}). Subsequently, the collected Os fraction was evaporated and converted to chloride by addition of 6-N HCl. Then, the concentrations of ^{188}Os and ^{190}Os were determined by measuring the mixture of the spike and a gravimetric standard solution of Os salt using the Carius tube method.[43] Finally, the double spike was created by mixing the ^{188}Os and ^{190}Os solutions according to their concentrations. The isotope compositions and concentration of double spikes were certified through the Carius tube method (Fig. 1).[43]

The disequilibrium of Os isotopes in mixed-spike solutions is likely attributed to valence discrepancies of Os species, as Os(IV) or Os(VI) can gradually oxidize to higher valence states even in reducing environments.[39] To investigate the homogeneity of Os solutions after chemical reduction, a mixed solution (3.5 μg g^{-1}) of ^{188}Os–^{190}Os and an Os salt standard was prepared for testing. Aliquots (1 μL) of the mixed solution were transferred into PFA beakers and combined with varying concentrations of reductant: 0.1 mol L^{-1} $NH_2OH \cdot HCl$, 0.01 mol L^{-1} $NH_2OH \cdot HCl$, and 0.05 mol L^{-1} $NH_2OH \cdot HCl$ + 0.01 mol L^{-1} HBr (Table S1). The mixtures were left at room temperature (22 °C) for natural evaporation to 1–2 μL before loading onto Pt filaments. The absolute volume ratios of the Os solution to reductant are given in Table S1 and Fig. 3. Additionally, the preservation state of the Os solution, with and without refrigeration, was compared to evaluate the effect of dissolved oxygen as a function of storage time.

Reference material WMS-1a was digested in reverse *aqua regia* under two conditions: (1) 220 °C for 48 h to obtain the
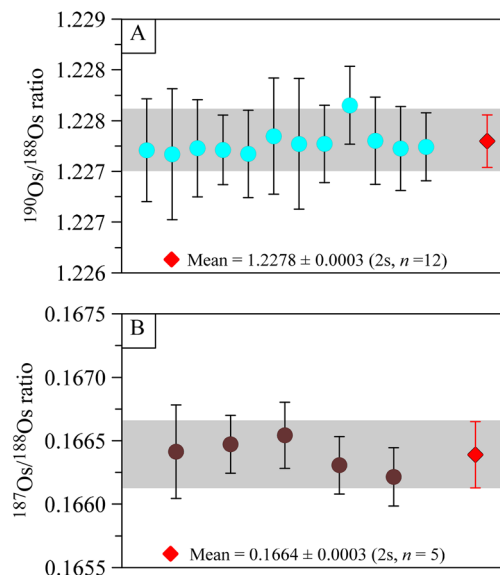
Fig. 1 Measurements of $^{190}Os/^{188}Os$ ratio for $^{188}Os-^{190}Os$ spike solutions (A), and $^{187}Os/^{188}Os$ ratio for reference material WMS-1a (B). Error bars for the cycles represent internal errors (± 2 s.e.) from 200 cycles of 4.19 second-integration periods, and the error bar for the rhombus represents the intermediate precision based on replicate measurements.

recommended ratio of $^{187}Os/^{188}Os$, and (2) 150 °C for 2 h to compare the $^{187}Os/^{188}Os$ ratio under different operational conditions. Powdered samples were spiked with Os, loaded into Carius tubes with 7.5 mL of reverse *aqua regia*, sealed, and digested at the specified temperature and duration. After cooling, solutions were decanted into centrifuge tubes containing 5 mL of CCl_4 for Os extraction, followed by HBr back-extraction. To evaluate isotopic equilibration efficiency under milder digestion conditions (150 °C, 2 h), the extracted Os was processed in three ways: (i) direct loading onto Pt filaments for measurement, (ii) purification by microdistillation only, and (iii) purification by combined chemical reduction and microdistillation. The progressive improvement in $^{187}Os/^{188}Os$ ratios during these steps demonstrates the method's effectiveness in achieving Os isotopic equilibration.

2.3 Mass spectrometry

2.3.1 Sample loading. The sample loading technique significantly influences the stability and intensity of Os ion beams. Prior to loading, Pt filaments were outgassed at ~3 A for 15 min under atmospheric pressure. To evaluate the impact of the loading method, several different sample loading techniques were tested. For the mixed $^{188}Os-^{190}Os$ spike solution, samples were loaded onto Pt filaments heated at an estimated 0.5 A (not a measured value) by rotating the adjustment knob to position the pointer between 0.4 A and 0.6 A, followed by the addition of 1 μL of NaOH–Ba(OH)$_2$ activator, and then heated to 2 A to enhance the sample–activator interaction (tests on 21st, 24th, 26th, 27th June, and 4th July). On 30th July, samples were loaded onto filaments at ~0.5 A, then placed in the source

chamber and reduced at 1500 mA under 1.5×10^{-7} mbar, and finally covered with the activator. Additionally, a micro-distillation procedure was applied on 4th July to test the effect of redox reaction on Os isotope equilibration. For the $^{188}Os-^{190}Os$ and Os salt mixture, the reductant was carefully treated for potential impurities. Samples were dried on filaments by gradual heating: the reductant was evaporated to dryness at 0.5 A, melted at 1.5 A and decomposed at 1.8–1.9 A until black smoke ceased. On 27th Dec, reductants were melted at 1.5 A to assess their effects. On 29th Dec, activators were melted at ~3.0 A to evaluate the impact of transient high heating on measurement results.

2.3.2 Thermal process for sample measurement. Osmium isotopic analysis was performed by N-TIMS at the State Key Laboratory of Geological Processes and Mineral Resources, China University of Geosciences, Wuhan, China. This equipment is equipped with nine Faraday cups with six 10^{11} Ω and three 10^{13} Ω amplified resistors. Masses of 234 ($^{186}Os^{16}O_3$), 235 ($^{187}Os^{16}O_3$), 236 ($^{188}Os^{16}O_3$), 237 ($^{189}Os^{16}O_3$), 238 ($^{190}Os^{16}O_3$), 240 ($^{192}Os^{16}O_3$) were set to the L2, L1, C, H1, H2, H3 cups, and 233 ($^{185}Re^{16}O_3$) was set to the L3 cup to evaluate the effects of $^{187}Re^{16}O_3$ on $^{187}Os^{16}O_3$. The gain calibration for the Faraday cups was performed daily to ensure accurate corrections for efficiency. Analysis was performed in the low-mass resolution mode and consisted of 10 blocks, each comprising 20 cycles with 4.19 s integration time per cycle followed by three seconds of idle time.

The sample filament was placed into the source chamber and high-purity oxygen was bled into the chamber with the pressure maintained at ~2.5×10^{-7} mbar when the vacuum was below 1.5×10^{-7} mbar. OsO_3^- ion currents can increase with oxygen partial pressure in the ion source – a phenomenon that does not affect isotope ratios in homogeneous solutions.[44] The general thermal process was as follows: the sample filament was first rapidly heated to 1700 mA at 300 mA min^{-1}, and then heated at 50 mA min^{-1} to 2000 mA. After focusing the $^{190}Os^{16}O_3$ ion beam, the filament was continuously heated at 10 mA min^{-1} until the intensity of the $^{190}Os^{16}O_3$ ion beam exceeded 0.8 V, at which point acquisition of Os isotope data began. Prior to every sample run, baseline measurements and peak centering, using individual masses 236 ($^{188}Os^{16}O_3$) and 238 ($^{190}Os^{16}O_3$), were carried out. The temperature program described above was used for sample measurements on all dates except 26th and 27th June, when initial filament heating was changed to rates of 200 and 100 mA min^{-1}, respectively, followed by rates of 20 mA min^{-1} and 5 mA min^{-1} to 2000 mA. A slow heating speed can theoretically prompt the reaction of high-valence Os species and residual Br$^-$.

2.3.3 Data process. Osmium isotope analyses using N-TIMS were conducted by measuring OsO_3^- ions. The measured intensities of OsO_3^- ions do not represent the true Os isotopic compositions due to (a) oxygen isotopic interferences, such as isobaric molecular ions (*e.g.*, $^{i-1}Os^{16}O_2^{17}O^-$ and $^{i-2}Os^{16}O_2^{18}O^-$ and $^{i-2}Os^{16}O^{17}O_2^-$), and (b) mass fractionation during the thermal ionization process.[45–47] Oxygen isotopic interferences were corrected using fixed ratios of $^{18}O/^{16}O = 0.002044$ and $^{17}O/^{16}O = 0.000375$, as established in previous studies.[48,49] Mass

fractionation was corrected using the double spike technique and the geometric iterative resolution method of Feng *et al.* (2015).[50]

3 Results and discussion

3.1 Results of Os equilibrium by the Carius tube method

The Carius tube acid digestion method was employed for isotopic equilibration between the analyte and spike under high-pressure/temperature conditions.[30] Solvent extraction was utilized to separate Os fraction from inverse *aqua regia*.[43] Measurement analysis yielded a statistically consistent $^{190}Os/^{188}Os$ ratio of 1.2278 ± 0.0003 ($2s$, $n = 12$; Fig. 1A), which was certified as the recommended value for the mixed ^{188}Os–^{190}Os spike solution. The reference material WMS-1a yielded a mean $^{187}Os/^{188}Os$ ratio of 0.1664 ± 0.003 ($2s$, $n = 5$; Fig. 1B; Table S2), which is in agreement with the reported value of 0.166777 ± 230 (2RSD, ppm).[46]

3.2 Disequilibrium of Os isotopes caused by valence discrepancies

Osmium isotope analysis of the mixed ^{188}Os–^{190}Os spike solution loaded directly onto Pt filaments revealed significant non-equilibrium isotope fractionation, as evidenced by substantial variability in $^{190}Os/^{188}Os$ ratios and incomplete correlation of $^{190}Os/^{188}Os$ and $^{192}Os/^{188}Os$ (Fig. 2). This fractionation persisted across multiple sample loading techniques and thermal process protocols. In HCl-dominated media, osmium predominantly exists as Os(IV) species (*e.g.*, H_2OsCl_6 and H_2OsBr_6 complexes), but progressive oxidation to higher valence states induces mass-independent isotope fractionation during measurements.[39] Crucially, this chemically-driven fractionation exceeds instrumental mass fractionation effects and cannot be adequately corrected through the conventional double spike technique.

Systematic investigations were conducted to mitigate valence-state discrepancies through optimized thermal protocols. Initial experiments (26–27th June) employing slower heating rates aimed to facilitate the equilibration between residual halides (Br⁻/Cl⁻) and higher-valent Os species. However,

Fig. 2 Correlations of $^{190}Os/^{188}Os$ and $^{192}Os/^{188}Os$ under different measurement conditions. See SI for specific measurement conditions. Error bar representation was precluded due to pronounced isotopic variations that dominated the analytical uncertainty range.

resultant $^{190}Os/^{188}Os$ ratios deviated significantly from the recommended values (Fig. 2), potentially attributable to oxygen influx into the source chamber during measurement. Subsequent comparative trials (30th July) under oxygen-free conditions ($<1.5 \times 10^{-7}$ mbar) yielded improved precision, though ratios remained statistically distinct from the recommended value (Fig. 2). While oxygen-free reduction reduced the degree of isotopic disequilibrium, complete equilibrium was not achieved. Consequently, uncorrectable mass-independent fractionation from the spike disequilibrium precludes accurate isotope ratio determination. This limitation prevents quantitative correlation between vacuum conditions and ratio deviations.

Microdistillation techniques, previously validated for Os isotopic equilibration in geological samples and spikes[26,51] were adapted for the synthetic spike solutions. The measurement results yielded a mean $^{190}Os/^{188}Os$ ratio of 1.2261 ± 0.002 ($n = 3$) for 3.5 ng Os aliquots (4th July), which exhibited a systematic 0.12% negative bias relative to the Carius tube method (Fig. 2), exceeding the <1‰ tolerance required for high-precision Re–Os geochronology. This discrepancy suggests that, although redox cycling protocols partially mitigate valence-related fractionation, complete isotopic equilibration remains elusive under current experimental conditions.

3.3 Equilibration of Os isotopes

The observed disequilibrium in Os isotope ratios within the mixed spike solution may originate from valence state heterogeneity among Os species.[39] Such redox variations induce significant mass-independent fractionation, which cannot be effectively normalized through conventional double-spike techniques. To mitigate this analytical artifact, strategic introduction of a reducing agent $NH_2OH \cdot HCl$ is recommended to maintain uniform tetravalent Os(IV) speciation, thereby achieving Os isotope equilibration under ambient conditions. Compared with alternative reductants, such as ascorbic acid and thiourea used in a previous study during ICP-MS analysis,[52] $NH_2OH \cdot HCl$ possesses a simpler molecular structure than organic reductants and decomposes readily at a lower temperature (150 °C) than that of thiourea (270 °C) and ascorbic acid (300 °C), thus preserving Os oxidization during the decomposing process.

3.3.1 Testing sample-to-reductant volumetric ratios. The initial reductant concentration was empirically established based on previous studies employing mixed stabilizing solutions containing variable concentrations of acetic acid, thiourea, and ascorbic acid for Os isotope analysis by ICP-MS.[52] Accordingly, a 0.1 mol L⁻¹ $NH_2OH \cdot HCl$ solution was selected to homogenize Os oxidation states in mixed solutions. The sample-to-reductant volumetric ratio proves critical for achieving Os valence uniformity and ensuring measurement accuracy by N-TIMS. Preliminary experiments were conducted to investigate ratios ranging from 1 : 1 to 1 : 4 (Fig. 3). The $^{190}Os/^{188}Os$ ratio at 1 : 1 (1.2195 ± 0.0021, $2s$, $n = 2$) deviated significantly from the recommended value (1.2278 ± 0.0003). In contrast, ratios of 1 : 2 (1.2284 ± 0.0011, $2s$, $n = 2$), 1 : 3 (1.2287
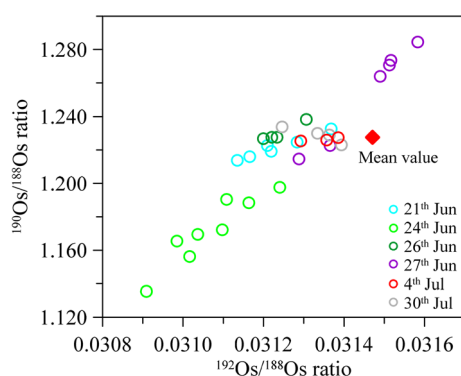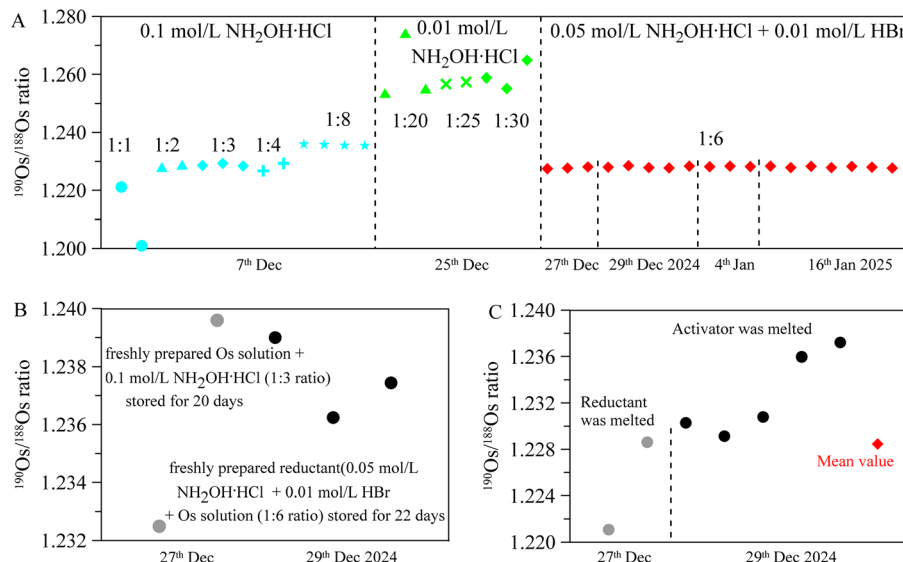
Fig. 3 (A) Measurements of $^{190}Os/^{188}Os$ under different combinations of samples and reductants, (B) effect of solution storage on measurement results, and (C) effect of sample loading technique using 0.05 mol L^{-1} NH$_2$OH·HCl + 0.01 mol L^{-1} HBr on measurement results. Error bar representation was precluded due to pronounced isotopic variations that dominated the analytical uncertainty range.

± 0.0009, 2s, n = 3), and 1 : 4 (1.2280 ± 0.0037, 2s, n = 2) yielded mean values concordant with the recommended value within measurement precision. These results demonstrate that ratios between 1 : 2 and 1 : 4 potentially stabilize Os valence states. The 1 : 3 ratio was adopted for subsequent experiments due to its superior intermediate precision, corresponding to a stoichiometric ratio of 3 × 10^{-7} mol NH$_2$OH·HCl per 3.5 ng Os during reduction.

3.3.2 Optimization of reductant concentration for Os isotope stabilization. The concentration of the reductant plays a critical role in Os isotope analysis. Excessively high concentrations increase Pt filament loading during thermal processing, whereas insufficient concentrations impede the reduction of high-valence Os species. To address this balance, we first systematically evaluated NH$_2$OH·HCl solutions at 0.01 mol L^{-1} with volumetric ratios of 1 : 20, 1 : 25, and 1 : 30. These trials consistently produced anomalously elevated $^{190}Os/^{188}Os$ ratios (Fig. 3A) that were attributable to two synergistic factors: (1) ambient temperature storage facilitated oxidation of Os(IV) to volatile OsO$_4$, resulting in irreversible isotopic fractionation; (2) suboptimal reductant concentration was insufficient for complete reduction of high-valence Os species. These hypotheses were subsequently validated through controlled comparative experiments.

A modified reductant system (0.05 mol L^{-1} NH$_2$OH·HCl + 0.01 mol L^{-1} HBr) demonstrated superior stabilization efficacy at a 1 : 6 stoichiometric ratio (3 × 10^{-7} mol NH$_2$OH·HCl per 3.5 ng Os). The inclusion of HBr provided dual advantages: (1) extended reaction kinetics through reduced volatility compared to aqueous media, and (2) enhanced redox potential for efficient Os species reduction. When applied to refrigerated (2 °C) freshly prepared solutions, this combination yielded $^{190}Os/^{188}Os$ ratios of 1.2277 ± 0.0006 (2s, n = 3) and 1.2281 ± 0.0007 (2s, n = 5) on 27th and 29th Dec, respectively (Fig. 3A). These values show

remarkable concordance with the recommended value and surpass the precision achieved with 0.1 mol L^{-1} NH$_2$OH·HCl alone at 1 : 3 ratio. Long-term reproducibility was further confirmed through replicate experiments on 4th and 16th January 2025, producing $^{190}Os/^{188}Os$ ratios of 1.2282 ± 0.0002 (2s, n = 3) and 1.2281 ± 0.0005 (2s, n = 6), respectively (Fig. 3A). This consistency verifies effective isotopic equilibration between ^{188}Os–^{190}Os spikes and Os salt solutions, as well as complete equilibration within inter-spike components (Fig. 4). The optional procedure yielded a mean value of 1.2280 ± 0.0006 (2s, n = 18), demonstrating close agreement with the recommended value of 1.2278 ± 0.0003 (2s, n = 12) obtained through the established Carius tube digestion method (Fig. 4). Although the intermediate precision of the optimized methodology
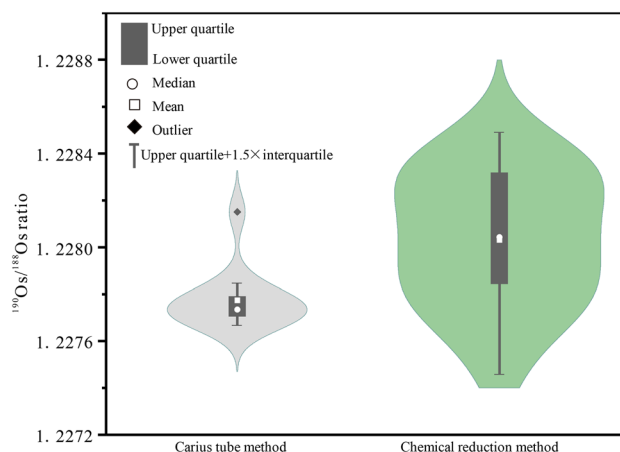

Fig. 4 Comparative results of $^{190}Os/^{188}Os$ ratio shown by the violin plot between (left) Carius tube and (right) chemically reducing reaction methods.

exhibits a marginal reduction relative to the conventional Carius tube protocol, the observed precision approaches the inherent instrumental uncertainty threshold ($\pm$0.0005, 2 s.e.) and validates methodological reliability for Re–Os isotopic dating requiring <1‰ analytical uncertainty. Additionally, Re–Os dating uncertainties for sulfide samples arise from spike concentration ($\sim$0.2‰) and Os measurement limitations due to low abundances in sulfides (typically >0.8‰). These combined uncertainties exceed the intermediate precision of the spike isotope ratios, thereby dominating the total analytical error budget.

The combination of the modified reductant with the Os mixed solution stored at room temperature for 22 days yielded a high $^{190}Os/^{188}Os$ ratio of 1.2376 $\pm$ 0.0023 (2s, $n = 3$, Fig. 3B) on 29th Dec, significantly deviating from the recommended value. This deviation suggests isotopic fractionation occurred due to volatile OsO_4 losses during prolonged storage at room temperature.[39] However, the ratio is lower than those obtained using 0.01 mol L^{-1} NH$_2$OH·HCl reductant, indicating an additional factor contributing to the isotopic offset. Based on direct measurements of the mixed ^{188}Os–^{190}Os spike solution (Fig. 2), the gradual valence change of Os species during the thermal process likely explains the observed large isotope fractionation.

3.3.3 Thermal processing effects on Os isotopic analysis.
The sample loading protocol involving sequential heating of the analyte and activator critically influences ion beam stability and induces detectable isotopic fractionation. Comparative experiments conducted on 27th Dec (Fig. 3C) revealed that partial melting of the reductant at a current of 1.5 A produced anomalous $^{190}Os/^{188}Os$ ratios (1.2211–1.2286), attributable to incomplete decomposition of NH$_2$OH·HCl accumulated on Pt filaments. Notably, Os hydroxide signals emerged at $\sim$1900 mA during the thermal process, matching the characteristic decomposition range of NH$_2$OH·HCl (1800–1900 mA). This implies that hydrogen ion generation primarily originates from reductant breakdown, compromising conventional oxygen interference corrections and consequently causing systematic isotopic deviations.

The activator heating step can also significantly affect the correction for Os isotope fractionation on N-TIMS. Our experimental design on 29th Dec employed gradually increasing electric current to 3 A to melt the activator, exceeding the optimal Os ionization threshold by $\sim$50%. The measurement results yielded elevated $^{190}Os/^{188}Os$ ratios (1.2291–1.2372, Fig. 3C), relating to the preferential loss of isotopically lighter volatile Os-oxides, consistent with mass-dependent fractionation mechanisms during the thermal process. As predicted by thermal ionization dynamics, the evaporation process causes increasing depletion of the lighter isotopes with increasing amounts of sample removed by evaporation,[53] and thus lighter isotopes (^{188}Os) exhibited enhanced volatility, leaving the isotopically heavier isotope (^{190}Os) for subsequent Faraday cup detection.

3.3.4 Procedural recommendations.
Fresh preparation of reducing agents proved critical for accurate Os isotope determination (Fig. 3B). Comparative experiments conducted on 7th and 27th Dec using identical 0.1 mol L^{-1} NH$_2$OH·HCl solutions revealed significant temporal degradation effects. The freshly prepared reductant (7th Dec) yielded $^{190}Os/^{188}Os = 1.2287 \pm 0.0009$ (2s, $n = 3$), statistically indistinguishable from the recommended value. In contrast, the aged reductant (20 day storage) produced an elevated mean ratio of 1.2360 $\pm$ 0.0100 (2s, $n = 2$, Fig. 3B), indicative of progressive oxidative degradation by dissolved O_2. This compromised redox capacity failed to maintain Os species in lower oxidation states, enabling valence-independent isotopic fractionation during the thermal process. While direct experimental evidence linking dissolved oxygen to NH$_2$OH·HCl oxidation is currently limited, multiple indirect pathways confirm its oxidative degradation. Dissolved O_2 oxidizes Fe^{2+} to/Fe^{3+}, which can cause the oxidation degradation of NH$_2$OH·HCl.[54] Consequently, we can reasonably infer that dissolved O_2 drives gradual NH$_2$OH·HCl degradation during storage, necessitating fresh preparation of the reductant solution prior to use.

Optimal reductant-to-analyte absolute volume ratios demonstrate controlled operational windows (Fig. 3A). Insufficient reductant addition (1 : 1 ratio, 7th Dec) resulted in incomplete Os species reduction, while excess reductant (1 : 8 ratio) caused Pt filament overloading, thus requiring more time for thermal decomposition of the reductant. Extended heating times caused a bias toward heavier isotope ratios, similar to the result when the activator was melted. In contrast, heating times insufficient for full decomposition of the reductant caused a bias toward lighter isotope ratios, similar to the result when the reductant was melted.

The maintenance of ultra-low reagent blanks is critical for high-precision Os isotope analysis of low-abundance geological materials such as pyrite. While NH$_2$OH·HCl cannot be subjected to pre-use purification, its application in the reduction protocol requires rigorous validation due to potential blank contributions. Quantitative analysis reveals that NH$_2$OH·HCl contains an Os concentration of 0.023 $\pm$ 0.006 pg g^{-1} (2s, $n = 3$), which represents a negligible contribution relative to typical Os concentrations in geological specimens. These findings demonstrate that NH$_2$OH·HCl not only facilitates effective spike–sample equilibration but also enables minimization of procedural blanks through its inherent low Os background.

3.4 Potential utilization of the developed methodology

The methodological development focused on resolving the critical challenge of spike–sample equilibration in Os isotopic analysis, which constitutes one of four major analytical limitations in this field.[18] Through systematic optimization, we established that controlled chemical reduction effectively stabilizes the uniform Os species. This stabilization was found to be essential for achieving complete isotopic equilibration between the ^{188}Os–^{190}Os spike and Os solution under ambient conditions, as demonstrated by long-term reproducibility during N-TIMS measurement (Fig. 4).

The developed method offers advantages with respect to both rapid equilibration between spike components and analysis of sulfide samples. Previous studies have demonstrated that Os equilibration between the sample and spike is critically
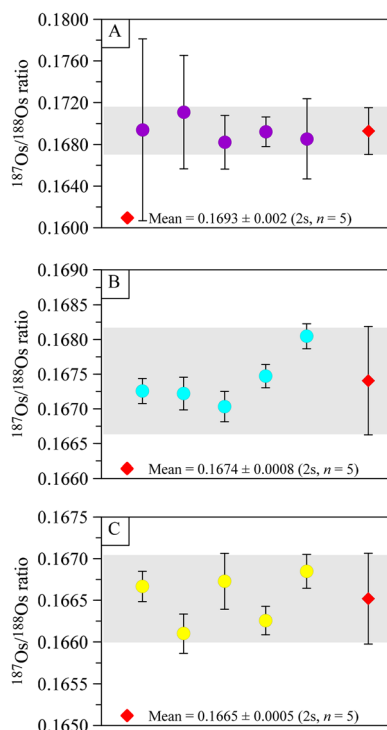
Fig. 5 $^{187}Os/^{188}Os$ ratios in replicates of the geological reference material WMS-1a for (A) solvent extraction, (B) solvent extraction combined with microdistillation, and (C) combination of solvent extraction, chemical reduction, and microdistillation, respectively, after digestion by reverse aqua regia at 150 °C for 2 hours. The error bars of the circles are internal errors (±2 s.e.) for 200 cycles of 4.19 second-integration periods, and the error bars for the rhombus represent the intermediate precision based on 5 times dependent replicate measurements.

dependent on digestion temperatures exceeding 200 °C and durations longer than 10 hours.[22,38] Consequently, it is evident that complete spike–sample equilibration was not achieved under conditions of 150 °C for 2 hours (Fig. 5A, B and Table S2). This is reflected in the replicate analyses (Fig. 5A), which show larger isotopic variations and yielded a mean $^{187}Os/^{188}Os$ value of 0.1693 ± 0.002 (2s, n = 5), which deviates significantly from the recommended value of 0.1664 ± 0.0003 (2s, n = 5; Fig. 1B). The larger analytical uncertainty (2 s.e.) observed is likely attributable to suppressed Os ion beam signals caused by matrix elements coextracted (e.g., Fe) with Os by the CCl_4 solvent. However, subsequent purification by microdistillation after solvent extraction effectively removed matrix interferences and potentially mitigated the disequilibrium effect. Analysis performed on 4th July 2024 (Fig. 2) of the $^{188}Os-^{190}Os$ ratio confirmed this improvement. Following microdistillation, the mean $^{187}Os/^{188}Os$ value improved to 0.1674 ± 0.0008 (2s, n = 5; Fig. 5B), approaching the recommended value. Furthermore, the optimal result, yielding a well-matched $^{187}Os/^{188}Os$ value of 0.1665 ± 0.0006 (2s, n = 5; Fig. 5C), was achieved using the combined purification steps of solvent extraction, chemical reduction, and microdistillation after sample digestion. These comparative experimental results demonstrate the efficacy of

our developed methodology for accurate Os isotope analysis of sulfide minerals.

The developed methodology demonstrates promising potential for streamlining sample pretreatment workflows in Os isotope analysis. Specifically, this approach enables precise double-spike Os isotopic measurements while eliminating the requirement for conventional Carius tube-based isotopic equilibration, thereby significantly reducing processing time by approximately 90% and consumable materials compared to traditional protocols. Critically, this lower reaction temperature (150 °C) substantially mitigates explosion hazards associated with digesting sulfide minerals compared to conventional high-temperature (>220 °C) approaches.

4 Conclusions

The optimized reductant system (0.05 mol L^{-1} NH$_2$OH·HCl + 0.01 mol L^{-1} HBr) demonstrated exceptional isotopic homogenization capacity between $^{188}Os-^{190}Os$ spikes and Os salts in this study. Notably, ambient-condition processing achieved $^{190}Os/^{188}Os$ ratios statistically indistinguishable from the Carius tube method. This breakthrough in the sample preparation protocol provides two key analytical advantages for low-abundance Os samples: (1) it is theoretically possible to reduce the procedural blank due to the reduced amount of reagent used, and (2) it reduces the explosion risk associated with the Carius tube as well as improving sample analysis efficiency, achieving complete Os isotope equilibration under relatively low temperature conditions and addressing critical challenges in Os isotope measurement via N-TIMS.

Conflicts of interest

There are no conflicts to declare.

Data availability

The authors confirm that all data supporting the findings of this study can be found within the manuscript.

Supplementary information is available. See DOI: **https://doi.org/10.1039/d5ja00151j**.

References

1 S. B. Shirey and R. J. Walker, *Annu. Rev. Earth Planet. Sci.*, 1998, **26**, 423–500.
2 S. J. Barnes and E. M. Ripley, *Rev. Mineral. Geochem.*, 2015, **81**, 725–774.

3 H. J. Stein, J. W. Morgan and A. Scherstén, *Econ. Geol.*, 2000, **95**, 1657–1671.

4 X. F. Zhao, M. F. Zhou, J. W. Li, D. Selby, X. H. Li and L. Qi, *Econ. Geol.*, 2013, **108**, 1489–1498.

5 L. I. Kemppinen, S. C. Kohn, I. J. Parkinson, G. P. Bulanova, D. Howell and C. B. Smith, *Earth Planet. Sci. Lett.*, 2018, **495**, 101–111.

6 J. Louis Birck and C. J. Allegre, *Earth Planet. Sci. Lett.*, 1994, **124**, 139–148.

7 I. S. Puchtel, A. D. Brandon, M. Humayun and R. J. Walker, *Earth Planet. Sci. Lett.*, 2005, **237**, 118–134.

8 E. R. V. Rocha-Júnior, I. S. Puchtel, L. S. Marques, R. J. Walker, F. B. Machado, A. J. R. Nardy, M. Babinski and A. M. G. Figueiredo, *Earth Planet. Sci. Lett.*, 2012, **337–338**, 164–173.

9 M. Sawamura, K. Kawai, Y. Matsuo, K. Kanie, T. Kato and E. Nakamura, *Nature*, 2002, **419**, 702–705.

10 D. G. Pearson, G. J. Irvine, D. A. Ionov, F. R. Boyd and G. E. Dreibus, *Chem. Geol.*, 2004, **208**, 29–59.

11 E. Rampone and A. W. Hofmann, *Lithos*, 2012, **148**, 247–261.

12 A. Sanfilippo, T. Morishita and R. Senda, *Geology*, 2016, **44**, 167–170.

13 J. T. Chesley and J. Ruiz, *Earth Planet. Sci. Lett.*, 1996, **154**, 1–11.

14 S. Jung, J. A. Pfänder, M. Brauns and R. Maas, *Geochim. Cosmochim. Acta*, 2011, **75**, 2664–2683.

15 W. T. Chen and M. F. Zhou, *Econ. Geol.*, 2012, **107**, 459–480.

16 Z. M. Zhu and Y. L. Sun, *Econ. Geol.*, 2013, **108**, 871–882.

17 D. Selby and R. A. Creaser, *Science*, 2005, **308**, 1293–1295.

18 H. Stein and J. Hannah in *Encyclopedia of Scientific Dating Methods*, Springer, New York, USA, 2014, ch. 36-1, pp. 1–25.

19 Z. K. Li, J. W. Li, H. S. Sun, X. F. Zhao, A. G. Tomkins, D. Selby, P. T. Robinson, X. D. Deng, Z. C. Wang, Z. Z. Yuan and S. R. Zhao, *Geol. Soc. Am. Bull.*, 2024, **136**, 277–294.

20 J. W. Mao, G. Q. Xie, F. Bierlein, W. J. Qü, A. D. Du, H. S. Ye, F. Pirajno, H. M. Li, B. J. Guo, Y. F. Li and Z. Q. Yang, *Geochim. Cosmochim. Acta*, 2008, **72**, 4607–4626.

21 N. J. Saintilan, D. Selby, R. A. Creaser and S. Dewaele, *Sci. Rep.*, 2018, **8**, 14946.

22 B. Zhao, X. Long, J. Li, A. Shen and X. He, *Geol. J.*, 2023, **58**, 3172–3180.

23 Z. Y. Chu, *Front. Chem.*, 2021, **8**, 615839.

24 L. Yin, P. P. Zhao, J. J. Liu and J. Li, *Earth-Sci. Rev.*, 2023, **238**, 104317.

25 A. Zimmerman, H. J. Stein, J. W. Morgan, R. J. Markey and Y. Watanabe, *Geochim. Cosmochim. Acta*, 2014, **131**, 13–32.

26 M. Paul, L. Reisberg and N. Vigier, *Chem. Geol.*, 2009, **258**, 136–144.

27 L. Qi and M. F. Zhou, *Geostand. Geoanal. Res.*, 2008, **32**, 377–387.

28 D. Malinovsky, I. Rodushkin, D. Baxter and B. Öhlander, *Anal. Chim. Acta*, 2002, **463**, 111–124.

29 L. Reisberg and T. Meisel, *Geostand. Newsl.*, 2007, **26**, 249–267.

30 S. B. Shirey and R. Walker, *J. Anal. Chem.*, 1995, **67**, 2136–2141.

31 T. Meisel, J. Moser, N. Fellner, W. Wegscheider and R. Schoenberg, *Analyst*, 2001, **126**, 322–328.

32 G. Ravizza and D. Pyle, *Chem. Geol.*, 1997, **141**, 251–268.

33 J. W. Morgan and J. M. Walker, *Anal. Chim. Acta*, 1989, **222**, 291–300.

34 R. Markey, J. L. Hannah, J. W. Morgan and H. J. Stein, *Chem. Geol.*, 2003, **200**, 395–406.

35 R. Markey, H. Stein and H. Morgan, *Talanta*, 1998, **45**, 935–946.

36 X. W. Huang, L. Qi, J. F. Gao, J. Hu and Y. Huang, *J. Anal. At. Spectrom.*, 2021, **36**, 64–69.

37 D. A. Du, D. Sun, S. Z, X. Wang, W. J. Qu and D. M. Zhao, *Rock Miner. Anal.*, 2002, **21**, 100–104.

38 L. Qi, M. F. Zhou, J. Gao and Z. Zhao, *J. Anal. At. Spectrom.*, 2010, **25**, 585–589.

39 H. He, A. Du, X. Zou, Y. Sun and N. Yin, *Chin. J. Anal. Chem.*, 1993, **22**, 109–114.

40 S. S. Fortenfant, D. B. Dingwell, W. Ertel-Ingrisch, F. Capmas, J. L. Birck and C. Dalpé, *Geochim. Cosmochim. Acta*, 2006, **70**, 742–756.

41 G. Yang, A. Zimmerman, H. Stein and J. Hannah, *Anal. Chem.*, 2015, **87**, 7017–7021.

42 R. Markey, H. J. Stein, J. L. Hannah, A. Zimmerman, D. Selby and R. A. Creaser, *Chem. Geol.*, 2007, **244**, 74–87.

43 D. Selby and R. A. Creaser, *Econ. Geol.*, 2001, **96**, 197–204.

44 T. Walczyk, E. H. Hebeda and K. G. Heumann, *Anal. Chem.*, 1991, **341**, 537–541.

45 J. A. M. Nanne, M. A. Millet, K. W. Burton, C. W. Dale, G. M. Nowell and H. M. Williams, *J. Anal. At. Spectrom.*, 2017, **32**, 749–765.

46 Z. Y. Chu, C. F. Li, Z. Chen, J. J. Xu, Y. K. Di and J. H. Guo, *Anal. Chem.*, 2015, **87**, 8765–8771.

47 A. Luguet, G. M. Nowell and D. G. Pearson, *Chem. Geol.*, 2008, **248**, 342–362.

48 R. Chatterjee and J. C. Lassiter, *Chem. Geol.*, 2015, **396**, 112–123.

49 T. Yokoyama, V. K. Rai, C. M. O. '. D. Alexander, R. S. Lewis, R. W. Carlson, S. B. Shirey, M. H. Thiemens and R. J. Walker, *Earth Planet. Sci. Lett.*, 2007, **259**, 567–580.

50 L. P. Feng, L. Zhou, L. Yang, S. Y. Tong, Z. F. Hu and S. Gao, *J. Anal. At. Spectrom.*, 2015, **30**, 2403–2411.

51 D. G. Pearson, S. B. Shirey, J. W. Harris and R. W. Carlson, *Earth Planet. Sci. Lett.*, 1998, **160**, 311–326.

52 K. V. Hoecke, C. Catry and F. Vanhaecke, *J. Anal. At. Spectrom.*, 2012, **27**, 1909–1919.

53 K. Habfast, *Int. J. Mass Spectrom.*, 1998, **176**, 133–148.

54 J. G. Wiederhold, N. Teutsch, S. M. Kraemer, A. N. Halliday and R. Kretzschmar, *Soil Chem.*, 2007, **71**, 1840–1850.